nature chemistry

ARTICLES

PUBLISHED ONLINE: 23 MAY 2016 | DOI: 10.1038/NCHEM.2518

Diindeno-fusion of an anthracene as a design strategy for stable organic biradicals

Gabriel E. Rudebusch[1], José L. Zafra[2], Kjell Jorner[3], Kotaro Fukuda[4], Jonathan L. Marshall[1], Iratxe Arrechea-Marcos[2], Guzmán L. Espejo[2], Rocío Ponce Ortiz[2], Carlos J. Gómez-García[5], Lev N. Zakharov[6], Masayoshi Nakano[4]*, Henrik Ottosson[3]*, Juan Casado[2]* and Michael M. Haley[1]*

The consequence of unpaired electrons in organic molecules has fascinated and confounded chemists for over a century. The study of open-shell molecules has been rekindled in recent years as new synthetic methods, improved spectroscopic techniques and powerful computational tools have been brought to bear on this field. Nonetheless, it is the intrinsic instability of the biradical species that limits the practicality of this research. Here we report the synthesis and characterization of a molecule based on the diindeno[*b,i*]anthracene framework that exhibits pronounced open-shell character yet possesses remarkable stability. The synthetic route is rapid, efficient and possible on the gram scale. The molecular structure was confirmed through single-crystal X-ray diffraction. From variable-temperature Raman spectroscopy and magnetic susceptibility measurements a thermally accessible triplet excited state was found. Organic field-effect transistor device data show an ambipolar performance with balanced electron and hole mobilities. Our results demonstrate the rational design and synthesis of an air- and temperature-stable biradical compound.

Biradical compounds push the covalent π bond to the limit of dissociation and yield highly reactive products. Owing to the strong π-electron correlation in these systems, new perspectives on the nature of the chemical bond are revealed and offer unique opportunities to investigate fundamental rules and concepts in chemistry. Organic compounds that exhibit a biradical character have been known since the early 20th century. A classic example is Tschitschibabin's hydrocarbon, first synthesized in 1907 (Fig. 1a)[1]. The compound features two linked dearomatized benzene rings. At the expense of a C=C double bond, the central rings regain aromaticity, which leads to an open-shell biradical structure that is in resonance with the closed-shell quinoidal structure[2]. The contribution of the open-shell resonance form to the overall ground-state structure is described by the biradical character index, y, which is derived from the natural orbital occupation number of the lowest unoccupied natural orbital[3,4]. The index ranges from pure biradical, $y = 1$, to pure closed shell, $y = 0$ (Fig. 1b). The interacting pair of electrons in open-shell polycyclic hydrocarbons (PCHs) can be in a spin-paired singlet state ($S = 0$) or a spin-parallel triplet state ($S = 1$)[5]. Owing to the double-spin polarization effect, most biradical PCHs have singlet ground states and low-lying triplet excited states[6]. Recent reports of compounds with quinoidal motifs and low-lying triplet states are illustrated in Fig. 1c[7–10]. Although represented with closed-shell bonding patterns, the compounds exhibit significant open-shell character ($y = 0.50$–0.74 (calculated at the PUHF (projected unrestricted Hartree–Fock)) level to permit comparison) with thermally accessible triplet states ($\Delta E(S_0 \rightarrow T_1) = 3.8$–$4.9$ kcal mol^{-1}) (Supplementary Section 9.2). This class of molecules has been shown to possess desirable properties, such as narrow frontier-orbital energy gaps[11], strong absorption in the visible spectrum, redox amphoterism, multicentre bonding, large second hyperpolarizabilities[12–15] and substantial two-photon absorption cross-sections[16,17]. There has been an effort towards taking advantage of biradical PCHs in nonlinear optics[15], molecular spintronics[18] and organic photovoltaic devices sensitized by singlet fission[19–21].

The practical application of open-shell PCHs has been hampered by the lack of stable and easily accessible materials. Indeed, the design and synthesis of stable open-shell organic compounds is challenging because of the reactivity associated with a biradical character and the inherent thermodynamic instability of pro-aromatic fragments. A survey of the literature is illustrative; recent examples of biradical PCHs suffer from protracted, low-yielding syntheses, decomposition under ambient conditions and insufficient characterization. Here we report the synthesis, characterization and properties of a new biradical PCH, diindeno[*b,i*]anthracene (**DIAn**). The synthesis is concise and possible on the gram scale. Our results are underlined by the remarkable stability of **DIAn** under ambient conditions and at elevated temperatures, and by the investigation of a low-lying triplet excited state through variable-temperature techniques. We offer a design strategy towards building biradical PCHs that approach the open-shell character of large acenes[22] but retain chemical stability. This work introduces new perspectives on the accessibility of high-spin organic materials with a view towards potential materials applications.

Results and discussion

Our approach to the synthesis of a stable diindenoanthracene derivative blocks the anticipated sites of high spin with bulky mesityl (Mes (2,4,6-trimethylphenyl)) groups. The introduction of (triisopropylsilyl)ethynyl groups from the outset provides solubility, steric bulk and resistance towards oxidation[23,24]. The synthesis is initiated by the palladium-catalysed Suzuki–Miyaura cross-coupling of the known dibromoanthracene **1**[25] and 2-formylbenzeneboronic acid (Fig. 2).

[1]Department of Chemistry & Biochemistry and the Materials Science Institute, University of Oregon, Eugene, Oregon 97403-1253, USA. [2]Department of Physical Chemistry, University of Malaga, Campus de Teatinos s/n, 229071 Malaga, Spain. [3]Department of Chemistry – BMC, Uppsala University, Box 576, Uppsala 751 23, Sweden. [4]Department of Materials Engineering Science, Graduate School of Engineering Science, Osaka University, Toyonaka, Osaka 560-8531, Japan. [5]Instituto de Ciencia Molecular, Universidad de Valencia, 46980 Paterna, Valencia, Spain. [6]CAMCOR, University of Oregon, Eugene, Oregon 97403-1433, USA. *e-mail: haley@uoregon.edu; casado@uma.es; mnaka@cheng.es.osaka-u.ac.jp; henrik.ottosson@kemi.uu.se

© 2016 Macmillan Publishers Limited. All rights reserved

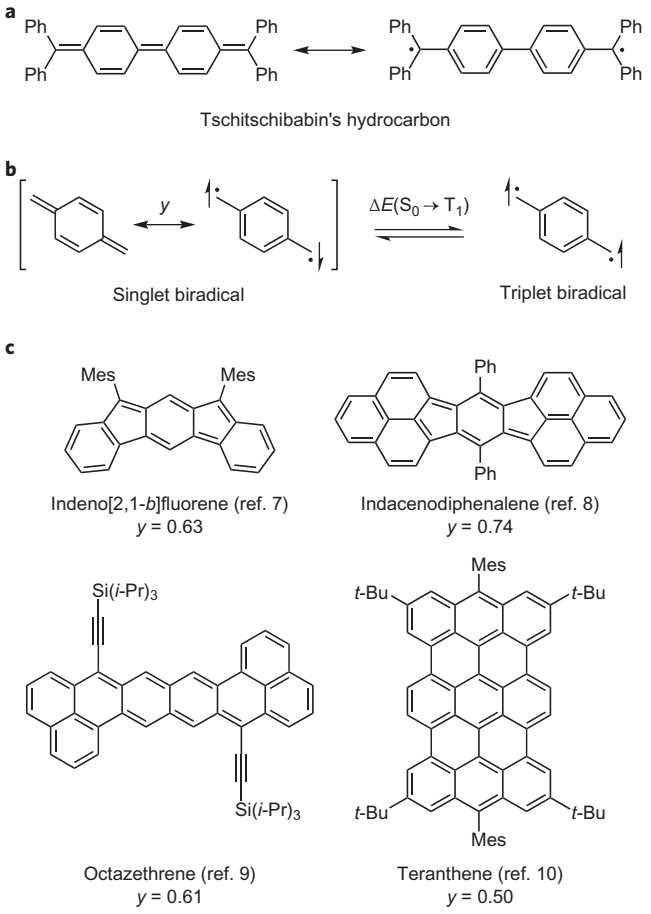

Figure 1 | PCHs with open-shell character. a, Molecular structure of Tschitschibabin's hydrocarbon, first synthesized in 1907, which illustrates the resonance between the closed-shell and open-shell structures. **b**, The electronic structure of open-shell PCHs is described by the biradical character index, *y*, and the energy difference between the singlet ground state and first triplet excited state, $\Delta E(S_0 \rightarrow T_1)$. **c**, Recent examples of compounds with significant open-shell character and thermally accessible triplet states. The biradical character (*y*) was calculated at the PUHF level to allow relevant comparisons (Supplementary Section 9.2).

The use of Buchwald's SPhos (2-dicyclohexylphosphino-2′,6′-dimethoxybiphenyl) ligand allows access to dialdehyde **2** in a near-quantitative yield. The addition of mesitylmagnesium bromide (MesMgBr) provides the secondary alcohol in high yield, which is carried forward without purification. Formation of the heptacyclic core of **3** was achieved through a Friedel–Crafts alkylation mediated by boron trifluoride etherate in 79% yield. Gratifyingly, selective closure to the C(3) and C(7) positions was observed because of the steric clash between the bulky Mes and Si(*i*-Pr)$_3$ groups that block electrophilic substitution at the more-activated C(1) and C(5) positions. Oxidation of the tertiary C–H bonds in **3** with DDQ (2,3-dichloro-5,6-dicyanobenzoquinone) provides the deep-violet **DIAn** in 62% yield. The synthetic route is possible on a moderate scale with 1 g of **3** prepared in a single sequence without chromatography. **DIAn** can be stored as a crystalline solid on the bench top, exposed to ambient conditions, without degradation. The half-life of a 10^{-6} M solution is approximately 64 days (Supplementary Fig. 1).

DIAn exhibits an electronic absorption spectrum similar to those of other quinoidal PCHs. The deep-blue colour of **DIAn** in solution can be ascribed to an absorption at 690 nm that extends into the green and red regions of the visible spectrum (Fig. 3a). The λ_{max} is significantly red shifted by 175 nm compared with the similar indeno[1,2-*b*]fluorene derivative[26]. The strong 690 nm absorption can be assigned to a symmetry-allowed $S_0 \rightarrow S_2$ transition with a weak shoulder that extends to 900 nm in the near infrared because of the symmetry-forbidden $S_0 \rightarrow S_1$ transition. Cyclic voltammetry (CV) reveals the amphoteric redox character of **DIAn** (Fig. 3b). Electron-accepting behaviour is evident in two reversible one-electron reductions at –1.28 and –1.67 V versus the ferrocene/ferrocenium couple (Fc/Fc^+). Although the ability of cyclopenta-fused PCHs to accept multiple electrons is established[26,27], **DIAn** is also easily oxidized in two one-electron oxidations at 0.17 and 0.70 V versus Fc/Fc^+. The full CV wave displays a striking symmetry between the oxidations and reductions, which indicates similar electrokinetic parameters for both anodic and cathodic processes. The highest occupied molecular orbital (HOMO) and lowest unoccupied molecular orbital (LUMO) energies, estimated from electrochemical data, are –5.27 and –3.82 eV, respectively. In conjunction with the 900 nm absorption edge, the HOMO/LUMO energy gap of 1.45 eV represents one of the narrowest values for a PCH that bears no strongly electron-withdrawing groups.

The amphoteric redox character of **DIAn** has implications for a balanced ambipolar charge transport[26]. In fact, organic field-effect transistors (OFETs) fabricated using octyltrichlorosilane-treated gate dielectrics by vapour deposition of **DIAn** gave ambipolar performances with quite balanced electron and hole mobilities. Analysis of these devices indicates a gradual increase of electron mobility with temperature at the expense of hole mobility; nevertheless, mobilities in the range 10^{-3}–10^{-2} cm^2 V^{-1} s^{-1} (Fig. 3c) were registered for the whole of the temperature range analysed (Supplementary Section 10). These values are comparable to the best values previously reported for organic biradicals[28,29]. However, of the many Kekulé biradicals reported in the literature, only a few are described as electrically active and, of these, a small fraction exhibit ambipolar behaviour. Rather, most exhibit a mismatched character between hole and electron mobilities, that is, unbalanced transport. In contrast, OFETs fabricated from **DIAn** result in an excellent performance in absolute simultaneous hole/electron mobilities with a unique balanced ambipolar

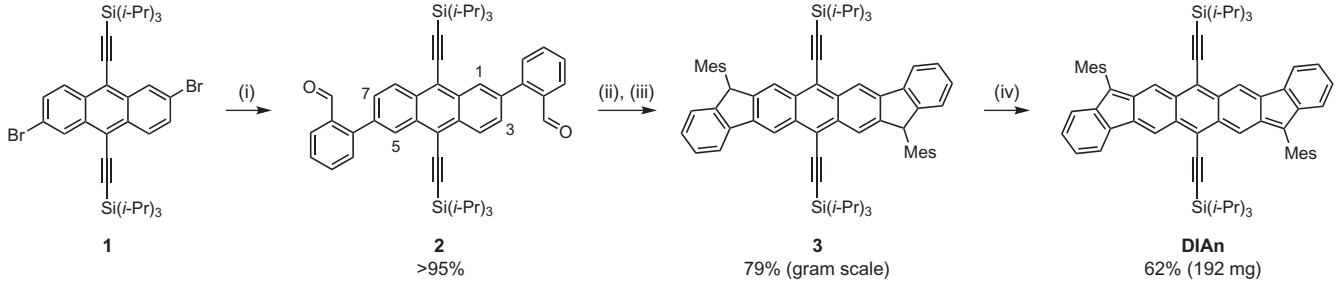

Figure 2 | Synthesis of DIAn. The synthetic route is rapid and efficient in four steps and 49% overall yield. Conditions: (i), 2-formylbenzeneboronic acid, $Pd(OAc)_2$, SPhos, K_3PO_4, toluene, 80 °C; (ii), MesMgBr, THF, 0 °C; (iii), $BF_3{\cdot}OEt_2$, CH_2Cl_2, 0 °C; (iv), DDQ, toluene, 80 °C.

© 2016 Macmillan Publishers Limited. All rights reserved

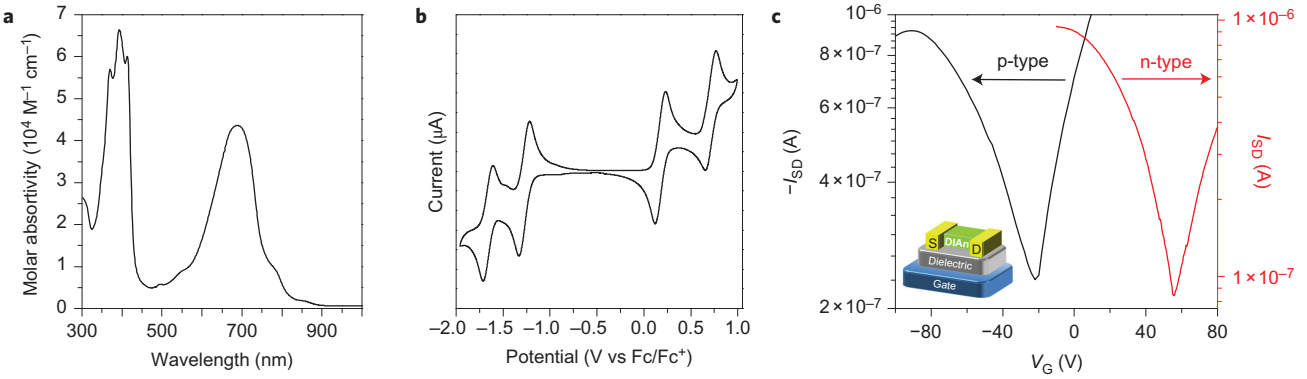

Figure 3 | Steady-state properties of DIAn and OFET device results. a, Electronic absorption spectrum of **DIAn** in CH_2Cl_2. **b**, CV of **DIAn** in CH_2Cl_2 shows two reversible one-electron reductions and two reversible one-electron oxidations with a HOMO/LUMO energy gap of 1.45 eV. **c**, OFET p-channel and n-channel transfer characteristics of a vapour-deposited film of **DIAn** exhibit balanced ambipolar charge transport. V_{SD} was fixed at 80 and -100 V for the positive and negative bias, respectively. μ_h (hole mobility) = 2×10^{-3} cm^2 V^{-1} s^{-1}; μ_e (electron mobility) = 4×10^{-3} cm^2 V^{-1} s^{-1}.

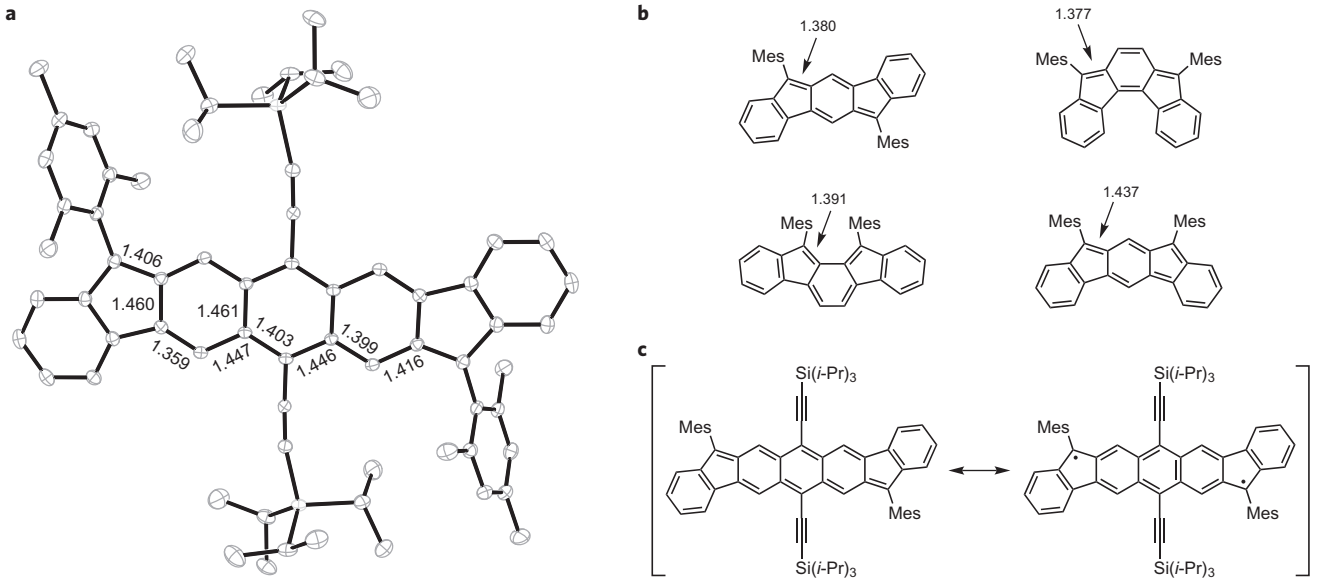

Figure 4 | Solid-state structure of DIAn by XRD. a, ORTEP image with selected bond distances (Å) of the **DIAn** core drawn with 35% thermal ellipsoids; hydrogens are omitted for clarity. **b**, In similar indeno-fused compounds, the bond distance from the apical carbon to the acene core is an indication of the degree of biradical character. **c**, The ground state of **DIAn** is a resonance hybrid between hypothetical closed-shell (left) and open-shell (right) structures.

transport. This device performance is aided by the chemical robustness of **DIAn** as the instability of many biradicals deteriorates the electrical response. In addition, the ambipolar behaviour can be explained by dual pseudoquinoidal (related to reduction and n-type transport) and pseudoaromatic (related to oxidation and p-type transport) structures acting in cooperation (see below).

Single-crystal X-ray diffraction (XRD) and bond-distance analysis provide insight into the ground-state electronic structure of PCHs. Prism-like crystals suitable for XRD were grown by slow diffusion of CH_3CN into a $CHCl_3$ solution of **DIAn**. The molecule is centrosymmetric and planar; the root mean squared deviation from an average plane drawn through the polycyclic core amounts to 0.03 Å. The outer six-membered rings have an average bond distance of 1.40 ± 0.01 Å, which indicates a benzenoid character. In the core of the molecule, significant bond-distance alternation is observed, as expected for a closed-shell quinoidal structure (Fig. 4a). The bond distances vary greatly, and span distances (1.359–1.461 Å) typically seen for double, benzenoid and single C–C bonds. On closer inspection of the quinoidal unit, significantly lengthened C–C bonds of 1.406 and 1.399 Å are apparent, which suggests a delocalized partial double-bond character rather than distinct double bonds. The bond distance from the apical sp^2 carbon to the anthracene core is 1.406 Å, whereas the analogous bond distances in the Mes-substituted indenofluorene isomers range from 1.377 Å (closed shell) to 1.437 Å (open shell) (Fig. 4b)[30]. The intermediate value in **DIAn** indicates contributions from both pure open-shell and closed-shell structures; thus, the solid-state structure of **DIAn** obtained at 173 K is a resonance hybrid in which both forms contribute to the overall ground electronic state (Fig. 4c).

More evidence for the unusual electronic structure of **DIAn** is brought to light by ^{1}H NMR experiments. Slightly broadened resonances are observed at 25 °C (Fig. 5a). As the temperature is increased to 150 °C in degassed 1,2-dichlorobenzene-d_4 the aromatic resonances broaden and eventually disappear. The signals are recovered to full height when the sample is cooled to 25 °C. Further cooling to –25 °C in CD_2Cl_2 allows the complete assignment of the ^{1}H resonances. The variable-temperature NMR studies suggest that a thermally accessible triplet state is responsible for the signal broadening. Interestingly, the presence of oxygen broadens the NMR spectra of **DIAn** (Supplementary Fig. 2). It can be inferred that $^3O_2$

© 2016 Macmillan Publishers Limited. All rights reserved

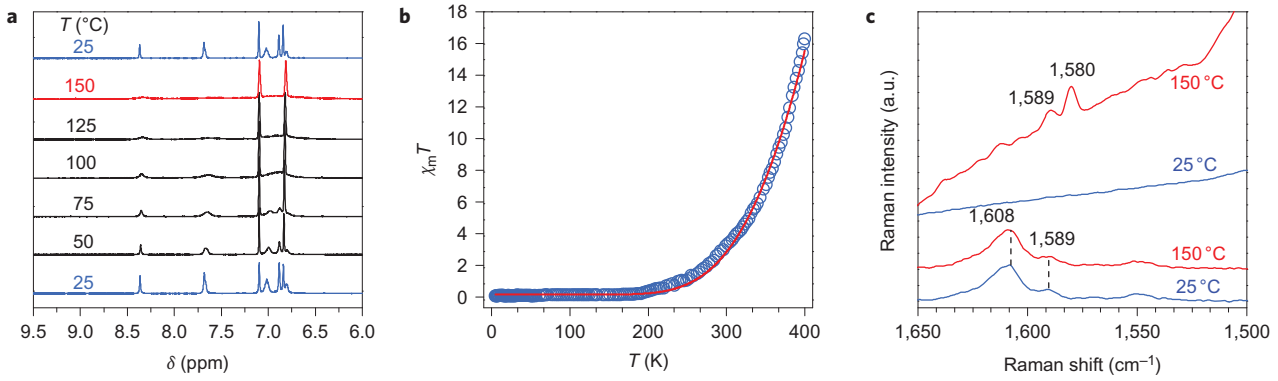

Figure 5 | Temperature-dependent properties of DIAn. a, The variable-temperature ^{1}H NMR experiment (500 MHz, 1,2-dichlorobenzene-d_4) shows broadening of the aromatic proton resonances with increasing temperature and the return of the original spectrum when cooled. **b**, SQUID measurements (blue circles) of the magnetic susceptibility, $\chi_m T$, from 4 to 400 K provide an estimation of $\Delta E(S_0 \rightarrow T_1)$ through fitting (red line) to the Bleaney–Bowers equation. **c**, Raman spectra (top, 785 nm; bottom: 633 nm) of **DIAn** from 25 to 150 °C show the formation of a new anthracene-like feature at elevated temperature. a.u., arbitrary units.

promotes reversible spin-crossover rather than engaging **DIAn** in an irreversible reaction[31]. This behaviour is in sharp contrast to that of most biradical PCHs, which readily decompose when heated or exposed to oxygen.

The magnetic properties of **DIAn** were studied by superconducting quantum interference device (SQUID) magnetometry and electron-spin resonance (ESR) spectroscopy. Figure 5b displays the SQUID magnetic response of **DIAn** ($\chi_m T$) from 4 to 400 K, which reveals a continuous increase of the whole magnetic molar susceptibility. The data can be fitted to the Bleaney–Bowers equation[32] and yields a low-to-high spin energy gap, $\Delta E(S_0 \rightarrow T_1)$, of 4.18 kcal mol^{-1}. This magnetic behaviour is also associated with a weak Q-band ESR absorption at a g of ~2.012 that decreases with cooling (Supplementary Fig. 12). Quantum chemical calculations using the spin-flip TD-PBE50 method with a non-collinear kernel[33] on the model **DIAn-a** (*vide infra*) gives a $\Delta E(S_0 \rightarrow T_1)$ of 4.9 kcal mol^{-1}, in good agreement with SQUID and ESR measurements (Supplementary Section 9.2). Taken together, this behaviour indicates antiferromagnetic coupling in the ground electronic state and a thermally activated ferromagnetic interaction between the π electrons of a triplet species populated by heating from the singlet ground state via intersystem crossing.

To investigate the transformation in molecular structure from singlet to triplet on heating, we turned to Raman spectroscopy[34,35]. The 1,064 nm Raman spectrum, which is very simple despite being recorded in non-resonant conditions, is dominated by two bands at 1,610 and 1,592 cm^{-1} that arise from C–C stretching vibrations of conjugated systems (Supplementary Fig. 8). The appearance of two ν(C=C) bands separated by ~20 cm^{-1} describes a situation in which there are distinct benzenoid and anthracene-like moieties in the conjugated core. This observation is in line with the solid-state structure of the singlet ground electronic state (Fig. 4c). Conversely, the 785 nm Raman spectrum at room temperature is featureless; however, with heating, a new band appears at 1,580 cm^{-1}, a value typical of anthracene derivatives[36]. Raman spectra of PCHs at temperatures above 50 °C are often strongly affected by the thermal effects on signal quality, which provokes the full disappearance of vibrational Raman bands. For **DIAn** we observed the opposite effect, a fact that can be addressed by considering the formation of an electronic state at a high temperature at the expense of a low-temperature configuration. The rather small $\Delta E(S_0 \rightarrow T_1)$ of 4.18 kcal mol^{-1} implies a thermal population of 2% for the triplet species at 150 °C, which justifies the detection by highly sensitive SQUID and ESR techniques. However, as this is also the case for the weak Raman signal, the phenomenon of Raman resonance must be invoked by which we observe the excited-state electronic absorptions of the triplet in the 785 nm spectrum at 150 °C[37]. Aside from a strict discussion of the magnitude of $\Delta E(S_0 \rightarrow T_1)$ in **DIAn**, it is clear that the process of populating the triplet state from the singlet state is statistically favourable, or entropy driven, an aspect already considered in the triply degenerate states in the Boltzmann equation. Indeed, entropy-driven effects have been invoked in singlet exciton fission to justify the fast singlet–triplet conversion under optical pumping of the excited electronic states in tetracene and pentacene[38]. It is interesting to consider that this situation in **DIAn** can be likened to an intramolecular entropy-driven singlet–triplet process. This may be viewed as a simplified situation in acene-like molecules of the more-complex singlet exciton fission process in which two neighbouring triplets are involved. Therefore, the fast singlet–triplet intersystem crossing in **DIAn** is fuelled by the favourable entropic conditions and by the small $\Delta E(S_0 \rightarrow T_1)$ because of the similarity of the singlet and triplet structures.

Quantum chemical calculations are a powerful tool to analyse the fragmental contributions to the π-electron structure of open-shell PCHs. To explore the properties of **DIAn** in more detail, we optimized two model compounds at the B3LYP/6-311G(d) level[39–41] (Fig. 6a). In **DIAn-a**, the large Si(i-Pr)$_3$ group is replaced with SiMe$_3$, and the Mes group is reduced slightly by one methyl, whereas in **DIAn-b** all the substituents are omitted. Calculations of the model systems confirm that **DIAn** has an open-shell singlet biradical ground state with the closed-shell singlet solution a modest 1.07 (**DIAn-b**) to 1.44 (**DIAn-a**) kcal mol^{-1} higher in energy. Calculations performed at the PUHF level on **DIAn-a** support this conclusion with $y = 0.62$, a value indicative of a moderate biradical character in the ground state[42]. As noted above, the greater stability of the singlet state compared with that of the triplet state results from the mechanism of double-spin polarization that preferentially stabilizes the singlet over the triplet solution[6]. Figure 6b shows the odd-electron density, a visualization of the biradical character index y, for the singlet open-shell state in which we observe densities primarily delocalized on the carbon atoms that link the outer benzenoid rings to the inner anthracene.

The ACID (anisotropy of the induced current density) method[43] is used to examine the ring currents at the CSGT-LC-UBLYP/6-311+G(d,p) level[44–47] in **DIAn-a** (Fig. 6c). Three well-differentiated diatropic (aromatic) circuits exist for the singlet open-shell ground state, the strongest in the external benzenoid rings, and a weaker anthracenic core, which is consistent with moderate open-shell character. The ACID plot for the triplet (Supplementary Fig. 19) reveals a markedly aromatic anthracene moiety, a prediction that

© 2016 Macmillan Publishers Limited. All rights reserved

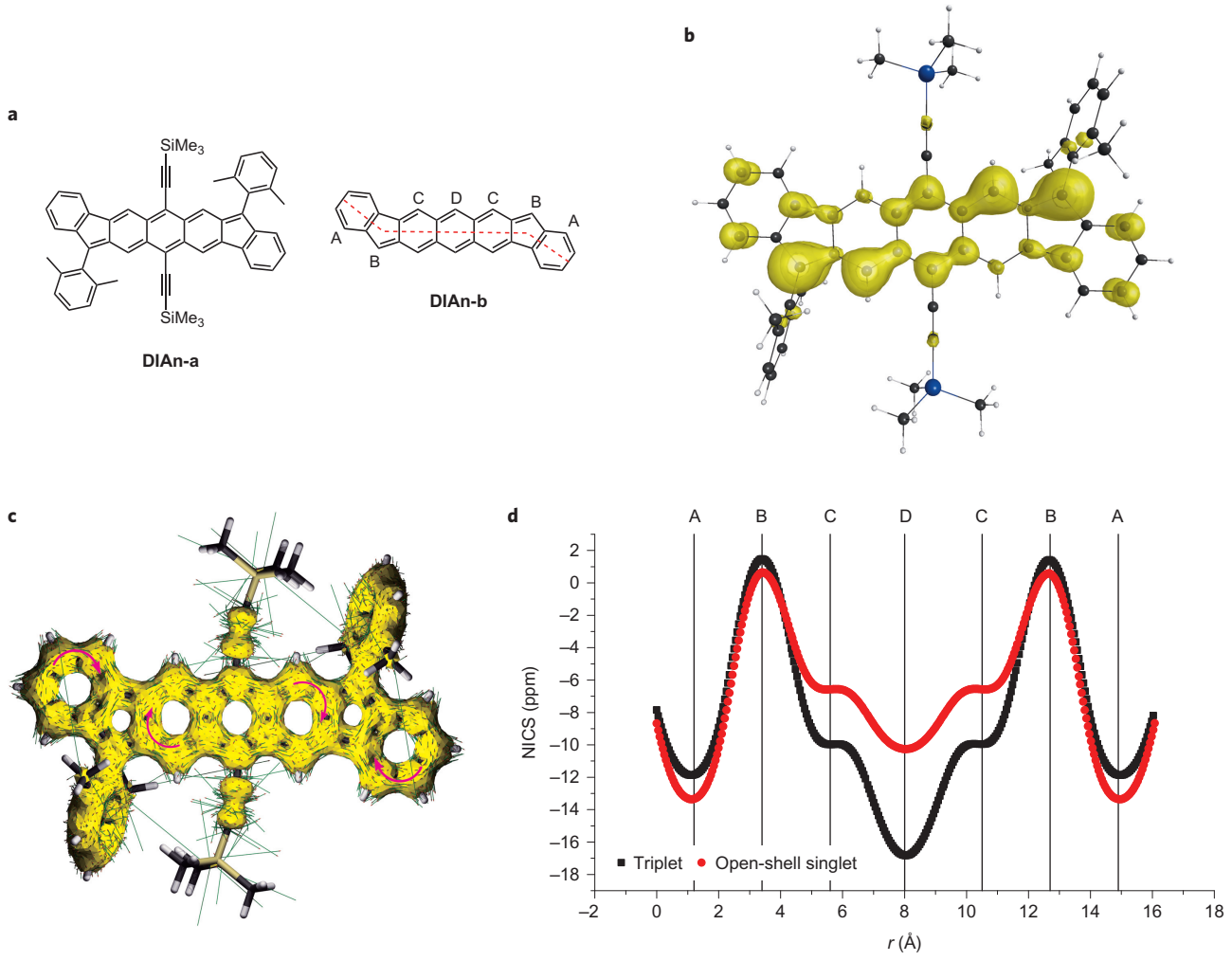

Figure 6 | Theoretical assessment of DIAn. a, Chemical structures of model systems **DIAn-a** and **DIAn-b**. **b**, The singlet biradical character of **DIAn-a** is visualized by the odd-electron density plot at a 0.001 a.u. isosurface value at the LC-UBLYP/6-311+G(d,p) level of theory. **c**, Isosurface (yellow) and current density vectors (green lines) calculated by ACID for the open-shell singlet state of **DIAn-a**. The general aromatic current is indicated by the superimposed clockwise magenta arrows. **d**, NICS-*XY* scans of the open-shell singlet and triplet states of **DIAn-b** show an increase in aromaticity for the thermally accessible triplet state. Capital letters (top) refer to the rings in the model structure in **a** and variable *r* describes the distance along the dashed red path.

justifies the appearance of the new Raman band at 1,580 cm^{-1} in the excited triplet state at lower frequencies (that is 1,590 cm^{-1}) than those of the weakly aromatized anthracene moiety in the singlet ground state.

The nucleus-independent chemical shift (NICS)-*XY* scan (Fig. 6d) of **DIAn-b** visually discloses the evolution of the NICS values along the different fragments of the molecular scaffold[48]. The GIAO-LC-UBLYP/6-311+G(d,p)[49] NICS values are taken 1.7 Å above the molecular plane and employ the σ-only model[50] to consider only the π contributions. The three minima correspond to the three aromatic parts of the molecule, the two external benzenes and the central anthracene, and more positive NICS values indicate a less-aromatic character. The open-shell singlet shows aromatic outer benzenoid rings and a somewhat aromatic anthracene core. In the triplet state the external benzenoid rings remain aromatic and the aromaticity of the central anthracene is accentuated. The two five-membered rings in both singlet and triplet states are non-aromatic and contain the sites of the highest odd-electron density, which further supports the resonance structures depicted in Fig. 4c.

Conclusions

In conclusion, we report here a new heptacene-like PCH that is segmented by two five-membered rings, and thus creates a central dearomatized anthracene. The diindenoanthracene is able to develop biradical character by the aromatization of a closed-shell, non-aromatic quinoidal structure. The significant results from this study are: (1) whereas acenes and related PCHs express biradical character and concomitantly acquire great reactivity and chemical instability, **DIAn** combines moderate biradical character with a chemical robustness, even in the presence of oxygen and at elevated temperatures; (2) the synthesis is concise, straightforward and multigram scalable, and so provides a versatile way to overcome a critical limitation of many biradical PCH syntheses. Undoubtedly, these are crucial aspects chemists must solve for the future use of these molecules in market-competitive applications. A complete characterization of the **DIAn** molecule is provided by single-crystal XRD, CV, optical and vibrational spectroscopies, magnetic measurements and quantum chemical calculations. We provide evidence for the singlet biradical ground electronic state with a thermally accessible triplet excited state. The rather small (4.18 kcal mol^{-1}) singlet–triplet gap is significant as the low value implies the ability of switching on and off the magnetic response in a reversible heating–cooling cycle. We scrutinized computationally the electronic structure of **DIAn** and explained the thermal behaviour as the result of the efficient intersystem crossing in a heavy-atom-free all-carbon molecule. The preparation of **DIAn** opens the way for a new family of

© 2016 Macmillan Publishers Limited. All rights reserved

five-membered-ring intercalated acenes in which chemical stability and biradical character are realized in concert. Based on these properties, and on preliminary OFET devices that yield balanced, ambipolar charge-transport behaviour, **DIAn** thus substantiates a strategy to optimize chemical design and engineering applications, which provides the foundation for the future use of these multifunctional molecules. We are now developing diindeno-fused tetracene and pentacene derivatives that will constitute the next step in the progress of obtaining organic materials with potential applications.

Methods

Synthesis of dialdehyde 2 by the Suzuki–Miyaura reaction. To a 100 ml unregulated pressure vessel equipped with a magnetic stir bar was added compound **1** (1.50 g, 2.15 mmol), 2-formylbenzeneboronic acid (0.81 g, 5.38 mmol, 2.50 equiv.), K_3PO_4 (1.25 g, 6.5 mmol, 3.00 equiv.) and toluene (25 ml). The mixture was sparged with N_2 for 20 minutes and then palladium(II) diacetate (10 mg, 0.043 mmol, 2 mol%) and SPhos (35 mg, 0.086 mmol, 4 mol%) were added and the mixture was sparged with N_2 for ten minutes. The vessel was sealed with a polytetrafluoroethylene cap and stirred at 80 °C for 18 hours. On cooling to room temperature, the reaction mixture was diluted with diethyl ether (50 ml) and washed with water (100 ml) and then brine (100 ml). The organic phase was dried over anhydrous magnesium sulfate and filtered. Removal of the volatiles under reduced pressure afforded **2** as an orange solid (1.60 g, >95%), melting point (m.p.), 226–227 °C; ^{1}H NMR (500 MHz, $CDCl_3$, 25 °C), δ (ppm) 10.18 (d, J = 0.8 Hz, 2H), 8.77–8.72 (m, 4H), 8.15 (dd, J = 7.9, 1.4 Hz, 2H), 7.77–7.70 (m, 4H), 7.67 (dd, J = 7.7, 1.2 Hz, 2H), 7.61 (t, J = 7.7 Hz, 2H), 1.24 (br s, 42H); ^{13}C NMR (126 MHz, $CDCl_3$, 25 °C), δ (ppm) 191.94, 145.38, 136.61, 133.83, 133.62, 132.36, 131.98, 131.06, 129.44, 128.77, 128.20, 128.03, 127.56, 119.19, 106.27, 102.68, 18.87, 11.45; high-resolution mass spectroscopy (HRMS) (ES^+) (m/z), calculated for $C_{50}H_{59}O_2Si_2$ $(M+H)^+$ 747.4048, found 747.4034; elemental analysis (EA), calculated for $C_{50}H_{58}O_2Si_2$, C 80.37%, H 7.82%, found C 80.38%, H 7.78%.

Synthesis of dihydro-DIAn 3. An oven-dried 100 ml flask equipped with a stir bar was charged with **2** (1.00 g, 1.34 mmol) and dry tetrahydrofuran (THF, 50 ml). The flask was cooled to 0 °C and then a THF solution of 2-MesMgBr (1M, 5.4 ml, 4.00 equiv.) was added via a syringe. After stirring for one hour, the reaction was quenched with saturated aqueous NH_4Cl solution (25 ml) and diluted with diethyl ether (50 ml). The organic phase was dried over anhydrous magnesium sulfate and filtered. Volatiles were removed under reduced pressure. The crude diol was dissolved in dry dichloromethane (150 ml) and cooled to 0 °C. Boron trifluoride diethyl etherate (0.66 ml, 5.4 mmol, 4.00 equiv.) was added dropwise and the dark solution was stirred for five minutes. With vigorous stirring, the excess catalyst was quenched by the addition of saturated aqueous $NaHCO_3$ solution (25 ml). The organic phase was concentrated under reduced pressure to 25 ml and then ethanol (25 ml) was added. The mixture was filtered and washed with water to provide **3** as a yellow solid (1.01 g, 79%); m.p., decomposition >330 °C; ^{1}H NMR (600 MHz, $CDCl_3$, 25 °C), δ (ppm) 9.03 (s, 2H), 8.41 (d, J = 1.6 Hz, 2H), 7.97 (d, J = 7.6 Hz, 2H), 7.47 (t, J = 7.4 Hz, 2H), 7.35 (t, J = 7.3 Hz, 2H), 7.31 (d, J = 7.5 Hz, 2H), 7.05 (d, J = 2.0 Hz, 2H), 6.67 (s, 2H), 5.81 (s, 2H), 2.74 (s, 6H), 2.32 (s, 6H), 1.22 (br s, 42H), 1.18 (s, 6H); ^{13}C NMR (151 MHz, $CDCl_3$, 25 °C), δ (ppm) 148.39, 146.67, 140.78, 140.03, 137.65, 137.44, 136.17, 134.31, 132.48, 132.16, 130.58, 128.87, 128.61, 127.20, 124.53, 121.42, 121.04, 118.27, 117.04, 104.25, 104.17, 49.28, 21.80, 20.88, 19.34, 18.86, 11.55; HRMS (ES^+) (m/z), calculated for $C_{68}H_{79}Si_2$ $(M+H)^+$ 951.5720, found 951.5726; EA, calculated for $C_{68}H_{78}Si_2$ C 85.83%, H 8.26%, found C 85.69%, H 8.18%.

Synthesis of DIAn. To a 250 ml flask with a stir bar was added **3** (310 mg, 0.26 mmol) and dry toluene (75 ml). The mixture was sparged with N_2 for ten minutes and then brought to 80 °C. On dissolution of **3**, DDQ (89 mg, 0.39 mmol, 1.50 equiv.) in toluene (5 ml) was added dropwise via a syringe. After stirring for three hours, the deep-blue solution was cooled then passed through a plug of basic alumina (4 × 8 cm), eluting with a 1:1 mixture of dichloromethane and hexanes. Volatiles were removed under reduced pressure. The crude material was dissolved in chloroform and an equal volume of acetonitrile was carefully layered above. Dark-violet blades of **DIAn** were collected by filtration (192 mg, 62%); m.p., decomposition >260 °C; ^{1}H NMR (600 MHz, CD_2Cl_2, –25 °C), δ (ppm) 8.41 (s, 2H), 7.72 (d, J = 6.3 Hz, 2H), 7.65 (s, 2H), 7.25–7.19 (m, 4H), 7.02 (s, 4H), 6.97 (d, J = 6.3 Hz, 2H), 2.39 (s, 6H), 2.09 (s, 12H), 1.11 (br s, 42H); ^{13}C NMR (151 MHz, CD_2Cl_2, –25 °C), δ (ppm) 143.87, 141.89, 138.94, 137.54, 136.85, 136.46, 135.37, 132.54, 130.31, 129.78, 128.73, 128.38, 126.77, 123.54, 123.06, 122.06, 121.58, 121.18, 105.80, 102.34, 21.08, 20.20, 18.53, 11.28; HRMS (ES^+) (m/z), calculated for $C_{68}H_{77}Si_2$ $(M+H)^+$ 949.5564, found 949.5536; EA, calculated for $C_{68}H_{76}Si_2$ C 86.02%, H 8.07%, found C 86.06%, H 8.03%.

Received 12 October 2015; accepted 21 March 2016; published online 23 May 2016

References

1. Tschitschibabin, A. E. Über einige phenylierte Derivate des p,p-Ditolyls. *Chem. Ber.* **40,** 1810–1819 (1907).
2. Montgomery, L. K., Huffman, J. C., Jurczak, E. A. & Grendze, M. P. The molecular structures of Thiele's and Chichibabin's hydrocarbons. *J. Am. Chem. Soc.* **108,** 6004–6011 (1986).
3. Doehnert, D. & Koutecky, J. Occupation numbers of natural orbitals as a criterion for biradical character. Different kinds of biradicals. *J. Am. Chem. Soc.* **102,** 1789–1796 (1980).
4. Yamaguchi, K. *et al.* Analytical and *ab initio* studies of effective exchange interactions, polyradical character, unpaired electron density, and information entropy in radical clusters (R)N: allyl radical cluster (N = 2–10) and hydrogen radical cluster (N = 50). *Int. J. Quantum Chem.* **90,** 370–385 (2002).
5. Abe, M. Diradicals. *Chem. Rev.* **113,** 7011–7088 (2013).
6. Karafiloglou, P. The double (or dynamic) spin polarization in π diradicals. *J. Chem. Educ.* **66,** 816–817 (1989).
7. Shimizu, A. *et al.* Indeno[2,1-*b*]fluorene: a 20-π-electron hydrocarbon with very low-energy light absorption. *Angew. Chem. Int. Ed.* **52,** 6076–6079 (2013).
8. Kubo, T. *et al.* Synthesis, intermolecular interaction, and semiconductive behavior of a delocalized singlet biradical hydrocarbon. *Angew. Chem. Int. Ed.* **44,** 6564–6568 (2005).
9. Li, Y. *et al.* Kinetically blocked stable heptazethrene and octazethrene: closed-shell or open-shell in the ground state? *J. Am. Chem. Soc.* **134,** 14913–14922 (2012).
10. Konishi, A. *et al.* Synthesis and characterization of teranthene: a singlet biradical polycyclic aromatic hydrocarbon having Kekulé structures. *J. Am. Chem. Soc.* **132,** 11021–11023 (2010).
11. Sun, Z., Ye, Q., Chi, C. & Wu, J. Low band gap polycyclic hydrocarbons: from closed-shell near infrared dyes and semiconductors to open-shell radicals. *Chem. Soc. Rev.* **41,** 7857–7889 (2012).
12. Nakano, M. *et al.* Second hyperpolarizability (γ) of singlet diradical system: dependence of γ on the diradical character. *J. Phys. Chem. A* **109,** 885–891 (2005).
13. Motomura, S. *et al.* Size dependences of the diradical character and the second hyperpolarizabilities in dicyclopenta-fused acenes: relationships with their aromaticity/antiaromaticity. *Phys. Chem. Chem. Phys.* **13,** 20575–20583 (2011).
14. Nakano, M. *et al.* Relationship between third-order nonlinear optical properties and magnetic interactions in open-shell systems: a new paradigm for nonlinear optics. *Phys. Rev. Lett.* **99,** 033001 (2007).
15. Nakano, M. & Champagne, B. Theoretical design of open-shell singlet molecular systems for nonlinear optics. *J. Phys. Chem. Lett.* **6,** 3236–3256 (2015).
16. Kamada, K. *et al.* Strong two-photon absorption of singlet diradical hydrocarbons. *Angew. Chem. Int. Ed.* **46,** 3544–3546 (2007).
17. Zeng, Z. *et al.* Pro-aromatic and anti-aromatic π-conjugated molecules: an irresistible wish to be diradicals. *Chem. Soc. Rev.* **44,** 6578–6596 (2015).
18. Morita, Y., Suzuki, S., Sato, K. & Takui, T. Synthetic organic spin chemistry for structurally well-defined open-shell graphene fragments. *Nature Chem.* **3,** 197–204 (2011).
19. Ito, S., Minami, T. & Nakano, M. Diradical character based design for singlet fission of condensed-ring systems with 4$n\pi$ electrons. *J. Phys. Chem. C* **116,** 19729–19736 (2012).
20. Smith, M. B. & Michl, J. Recent advances in singlet fission. *Annu. Rev. Phys. Chem.* **64,** 361–386 (2013).
21. Varnavski, O. *et al.* High yield ultrafast intramolecular singlet exciton fission in a quinoidal bithiophene. *J. Phys. Chem. Lett.* **6,** 1375–1384 (2015).
22. Thorley, K. J. & Anthony, J. E. The electronic nature and reactivity of the larger acenes. *Isr. J. Chem.* **13,** 642–649 (2014).
23. Anthony, J. E., Brooks, J. S., Eaton, D. L. & Parkin, S. R. Functionalized pentacene: improved electronic properties from control of solid-state order. *J. Am. Chem. Soc.* **123,** 9482–9483 (2001).
24. Fudickar, W. & Linker, T. Why triple bonds protect acenes from oxidation and decomposition. *J. Am. Chem. Soc.* **134,** 15071–15082 (2012).
25. Park, J.-H. *et al.* Soluble and easily crystallized anthracene derivatives: precursors of solution-processable semiconducting molecules. *Org. Lett.* **9,** 2573–2576 (2007).
26. Chase, D. T. *et al.* 6,12-Diarylindeno[1,2-*b*]fluorenes: syntheses, photophysics, and ambipolar OFETs. *J. Am. Chem. Soc.* **134,** 10349–10352 (2012).
27. Wood, J. D., Jellison, J. L., Finke, A. D., Wang, L. & Plunkett, K. N. Electron acceptors based on functionalizable cyclopenta[*hi*]aceanthrylenes and dicyclopenta[*de*,*mn*]tetracenes. *J. Am. Chem. Soc.* **134,** 15783–15789 (2012).
28. Chikamatsu, M. *et al.* Ambipolar organic field-effect transistors based on a low band gap semiconductor with balance hole and electron mobilities. *Appl. Phys. Lett.* **91,** 043506 (2007).
29. Koike, H. *et al.* Stable delocalized singlet biradical hydrocarbon for organic field-effect transistors. *Adv. Funct. Mater.* **26,** 277–283 (2016).
30. Marshall, J. L. & Haley, M. M. in *Organic Redox Systems: Synthesis, Properties and Applications* 1st edn (ed. Nishinaga, T.) 311–358 (Wiley, 2016).
31. Turro, N. J., Ramamurthy, V. & Scaiano, J. C. in *Principles of Molecular Photochemistry: An Introduction* 1st edn (University Science Books, 2009).

© 2016 Macmillan Publishers Limited. All rights reserved

32. Bleaney, B. & Bowers, K. D. Anomalous paramagnetism of copper acetate. *Proc. R. Soc. Lond. A* **214,** 451–465 (1952).
33. Bernard, Y. A., Shao, Y. & Krylov, A. I. General formulation of spin-flip time-dependent density functional theory using non-collinear kernels: theory, implementation, and benchmarks. *J. Chem. Phys.* **136,** 204103 (2012).
34. Casado, J. *et al.* Raman detection of 'ambiguous' conjugated biradicals: rapid thermal singlet-to-triplet intersystem crossing in an extended viologen. *Angew. Chem. Int. Ed.* **47,** 1443–1446 (2008).
35. Casado, J., Ponce Ortiz, R. & López Navarrete, J. T. Quinoidal oligothiophenes: new properties behind an unconventional electronic structure. *Chem. Soc. Rev.* **41,** 5672–5686 (2012).
36. Casado, J. *et al.* Vibrational fingerprint of the structural tuning in push–pull organic chromophores with quinoid or proaromatic spacers. *J. Chem. Phys.* **126,** 074701 (2007).
37. Albrecht, A. C. On the theory of Raman intensities. *J. Chem. Phys.* **34,** 1476–1484 (1961).
38. Burdett, J. J. & Bardeen, C. J. Quantum beats in crystalline tetracene delayed fluorescence due to triplet pair coherences produced by direct singlet fission. *J. Am. Chem. Soc.* **134,** 8597–8607 (2012).
39. Frisch, M. J. *et al. Gaussian 09, Revision D.01* (Gaussian, Inc., 2009).
40. Stephens, P. J., Devlin, F. J., Chabalowski, C. F. & Frisch, M. J. *Ab initio* calculation of vibrational absorption and circular dichroism spectra using density functional force fields. *J. Phys. Chem.* **98,** 11623–11627 (1994).
41. Krishnan, R., Binkley, J. S., Seeger, R. & Pople, J. A. Self-consistent molecular orbital methods. XX. A basis set for correlated wave functions. *J. Chem. Phys.* **72,** 650–654 (1980).
42. Yamaguchi, K. in *Self-Consistent Field: Theory and Applications* 1st edn (eds Carbó, R. & Klobukowski, M.) 727–828 (Elsevier, 1990).
43. Herges, R. & Geuenich, D. Delocalization of electrons in molecules. *J. Phys. Chem. A* **105,** 3214–3220 (2001).
44. Keith, T. A. & Bader, R. F. W. Calculation of magnetic response properties using a continuous set of gauge transformations. *Chem. Phys. Lett.* **210,** 223–231 (1993).
45. Becke, A. D. Density-functional exchange-energy approximation with correct asymptotic behavior. *Phys. Rev. A* **38,** 3098–3100 (1988).
46. Lee, C., Yang, W. & Parr, R. G. Development of the Colle–Salvetti correlation-energy formula into a functional of the electron density. *Phys. Rev. B* **37,** 785–789 (1988).
47. Iikura, H., Tsuneda, T., Yanai, T. & Hirao, K. A long-range correction scheme for generalized-gradient-approximation exchange functionals. *J. Chem. Phys.* **115,** 3540–3544 (2001).
48. Gershoni-Poranna, R. & Stanger, A. The NICS-*XY*-scan: identification of local and global ring currents in multi-ring systems. *Chem. Eur. J.* **20,** 5673–5688 (2014).
49. Wolinski, K., Hinton, J. F. & Pulay, P. Efficient implementation of the gauge-independent atomic orbital method for NMR chemical shift calculations. *J. Am. Chem. Soc.* **112,** 8251–8260 (1990).
50. Stanger, A. Obtaining relative induced ring currents quantitatively from NICS. *J. Org. Chem.* **75,** 2281–2288 (2010).

Acknowledgements

This work was supported by the US National Science Foundation (CHE-1301485), by the Spanish Government, MINECO (CTQ2012-33733 and CTQ2011-26507), by Junta de Andalucía (P09-FQM-4708) and Generalitat Valenciana (PrometeoII/2014/076), by a Japan Society for the Promotion of Science (JSPS) Research Fellowship for Young Scientists (No. 15J04949), Grant-in-Aid for Scientific Research (A) (No. 25248007) from the JSPS, a Grant-in-Aid for Scientific Research on Innovative Areas 'Stimuli-Responsive Chemical Species' (No. A24109002a), 'π-System Figuration' (15H00999), 'Photosynergetics' (A26107004a), the Strategic Programs for Innovative Research, Ministry of Education, Culture, Sports, Science & Technology, Japan, the Computational Materials Science Initiative, Japan, the Swedish Research Council (project grant 621-2011-4177) and the Swedish National Infrastructure for Computation (NSC, Linköping). K.J. and H.O. thank R. Herges for providing the AICD 2.0.0 program. The authors acknowledge the Biomolecular Mass Spectrometry Core of the Environmental Health Sciences Core Center at Oregon State University (NIH P30ES000210). We thank T. Kubo (Osaka) for insightful discussions.

Author contributions

G.E.R. conceived the project, and designed and carried out the experiments, analysed the data and wrote the manuscript. M.M.H. played a critical role in the discussion of the experimental design, project direction, experiments and results, and in the preparation of the manuscript. J.L.M. acquired and analysed the CV data. I.A.M., G.L.E. and R.P.O. obtained the OFET data. L.N.Z. acquired and analysed the X-ray crystallographic data. J.L.Z. performed the Raman spectroscopic measurements. C.G.G. performed the SQUID experiments. J.C. interpreted the magnetic and spectroscopic data and co-wrote the paper. K.F. and M.N. performed the calculation and discussed the geometry optimization, the open-shell character and the S–T gaps. K.J. performed the ACID and NICS-*XY* density functional theory calculations, and, together with H.O., analysed the data from these computations. All the authors discussed the results and commented on the manuscript.

Additional information

Supplementary information and chemical compound information are available in the online version of the paper. Reprints and permissions information is available online at www.nature.com/reprints. Correspondence and requests for materials should be addressed to M.N., H.O., J.C. and M.M.H.

Competing financial interests

The authors declare no competing financial interests.

© 2016 Macmillan Publishers Limited. All rights reserved